Integrated Assessment for the Deformation of Ground Surface and Tunnel Invert Induced Deep Excavation

Ahmed Kamal M. Ibrahim, *IAENG*, *Member*, Abd-Elaziz A. Senoon, Mamdouh Abbas Kenawi, Ahmed Rushdy Towfeek, Mostafa Abdo Abd- Elnaiem

Abstract—The surface deformation behind deep excavation support in sand soil was validated. Furthermore, the displacement of ground surface and invert of buried circular tunnel (diameter D = 6 m) induced by deep excavation in layered soft soil was evaluated. The validation was performed for the results of centrifuge models of sand soil by applying Mohr-Coulomb model (MC) in 2D finite element analysis. In addition, the evaluation was conducted for the MC model by applying Hardening Soil with Small Strain Stiffness (HSS) on a model in soft soils. Beginning an excavation in soft soils causes drawdown stresses that causing an abrupt increase in tunnel movement (strain dependent stiffness). MC model cannot adopt the effect of excavation increase on the surface of soft soil and on the invert of tunnel (under-predicted deformation). HSS adopts a steep drawdown for soft soil surface above the tunnel and indicates a marked decrease in the heave of tunnel invert (over-predicted deformation). According to the deformation of sand surface behind diaphragm wall of excavation, an accepted convergence was observed between the centrifuge sand tests and 2D numerical analysis.

Index Terms—Constructed facilities, constitutive model, linear elasticity, soil unloading, strain dependent stiffness.

I. INTRODUCTION

Tunnel construction can significantly affect buildings, utilities, and infrastructures, and vice versa [1]. Multiple case studies, e.g., [2]–[4] have performed accurate measurements of displacement. Numerical analysis is used in projects to evaluate the performance of the excavation system and ensure that the displacements are within tolerable limits, e.g., [5]–[7]. In-situ measurements and numerical simulations were used in [8] and it was reported that the proposed numerical model can account for the complexity of tunneling due to displacements. Finite element method (FEM) was used [9] to study the strength and stiffness parameters of soft clays with presenting an evaluation by the parameters of (MC) model and Hardening Soil model (HS). Extensive experimental tests were conducted [10] to obtain these parameters. MC model is a simple first analysis of the studied problem. Additionally, (HS) and (HSS) models require additional parameters such as reference secant stiffness (E_{50}^{ref}), reference unloading/reloading stiffness (E_{ur}^{ref}), and initial shear modulus (G_0) for the highly nonlinear behavior. HS and HSS models are applied to evaluate the results of model parameters and the effect on soil behavior. Recently, it was demonstrated [11] that HSS over-predicted heaves in excavation analyses. Furthermore, [12] applied MC, HS, HSS, and Soft Soil (SS) on soft clays to exhibit the settlement behind excavation support. Multiple researchers e.g., [10], [13]–[15] have applied constitutive models and centrifuge tests using different model parameters. Evaluating the obtained parameters (Laboratory or in-situ results) is costly and time-intensive. Only a few studies have validated the results of centrifuge tests or evaluated soil-structure models as an application for the assessment of facilities.

Therefore, an integrated assessment of the safety of facilities was conducted. From one side, the study puts an inclusive conceptualization for the effect of deep excavation on ground surface and from other side on tunnel invert. The study conducted 2D numerical analysis to validate a centrifuge model for Toyoura dry sand of Japan. The model analyzed tunnel close to deep excavation. In addition, the study applied a numerical model using the parameters of Bangkok soft clay (*Sukhumvit Station*) as a comprehensive evaluation study to illustrate the deformations of ground surface and tunnel invert (**Fig. 1**) due to strain-stiffness of soil. Conversely, this study handles an application on a wide range of integrated prediction for deformations that pose a severe effect on the efficiency of close facilities.

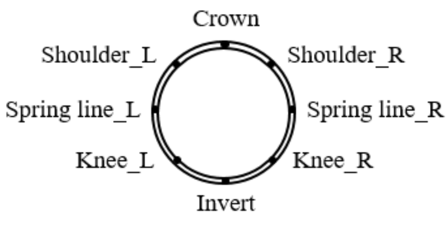

Fig. 1: The invert position of circular tunnel lining.

II. METHODS

A reliable validation for a case study of centrifuge model tests was provided. Two 3D centrifuge tests were conducted at the Hong Kong University of Science and Technology [15]. Several investigators, e.g., [15], [16] have evaluated the properties of Toyoura sand. Subsequently, the behavior of ground surface and tunnel invert induced excavation was investigated for a model of soft soils.

Manuscript received April 29, 2022, revised October 31, 2022.

Ahmed K. M. Ibrahim, member, IAENG, is a PhD Candidate in Civil Engineering Department, Faculty of Engineering, University of Assiut, Egypt, (corresponding author to provide phone: 0020-1013903102; (e-mail: mmraa.2008@gmail.com).

A. A. Senoon is a tenured professor in Civil Engineering Department, Faculty of Engineering, University of Assiut, Egypt. (e-mail: asenoon2000@yahoo.ca).

M. A. Kenawi is a tenured Assistant Professor in Civil Engineering Department, Faculty of Engineering, University of Sohag, Egypt. (e-mail: mkenawi2@yahoo.com).

A. R. Towfeek is a tenured Assistant Professor in Civil Engineering Department, Faculty of Engineering, Al-Azhar University, Egypt. (e-mail: ahmed_78_eng@yahoo.com).

M. A. Abd-Elnaiem is a tenured professor of Civil Engineering Department, Faculty of Engineering, University of Assiut, Egypt. (e-mail: mostafaabdo6689@gmail.com).

II.1. CENTRIFUGE TESTS AND RESULTS

The tests were prepared at a centrifugal acceleration of 60 g using a container with a length, width, and depth of 1245, 990, and 850 mm, respectively. The relevant scaling laws that were cited by [15] provide length of 74.7 m, width of 59.4 m, and depth of 51.0 m in prototype. The centrifuge modelling tested the effect of excavation on the ground surface of dry sand. In test (C), the excavation was conducted above the tunnel. In test (S), the excavation was located at a distance of 25 mm beside tunnel, **Fig. 2** (Redrawn based on Authors' idea). Representation of excavation by heavy fluid ($ZnCl_2$) that has the same density (γ) of sand was located in a flexible rubber bag. The excavation and penetration depths were 150 and 75 mm, respectively. Excavation was in three stages everyone was 50 mm (3 m in prototype). The vertical distance between the tunnel crown and formation level of the excavation was 50 mm (0.5D).

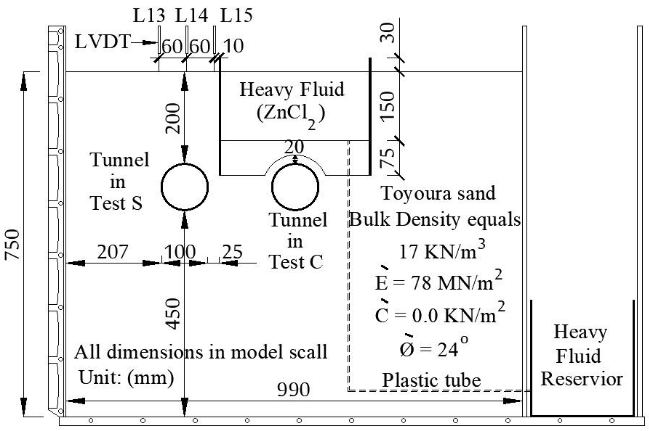

Fig. 2: Details of centrifuge model of Toyoura sand, (Redrawn based on Authors' idea).

II.1.1. SURFACE SETTLEMENT BEHIND RETAINING SYSTEM

The relationship between normalized ground surface settlement (δ_s/H_e) and normalized distance behind diaphragm wall (d/H_e) was illustrated in [15].

The results implied that no observed settlement in the surface of soil behind 1.15 H_e from the wall. This research verified the results of test C and S.

II.2. VALIDATING PROCEDURES FOR CENTRIFUGE MODEL

Two-dimensional numerical analysis was applied using the software package Plaxis 2D to perform back-analyses and verify the centrifuge test as a relationship between (δ_s/H_e) for the soil surface and normalized distance behind the wall (d/H_e). MC model was used to simulate the prototype model as drained. The length, width, and depth of the prototype centrifuge model were 74.7, 59.4, and 51.0 m. The depth of verification model was 60 m and the bulk density (γ_b) was 17 kN/m^3. The effective stiffness parameters ($\grave{E}$) and (ν) were 78 MN/m^2 and 0.2, respectively. In addition, the effective strength parameter ($\grave{Ø}$) was 24^o, and ($\grave{C}$) was zero. The excavation depth was simulated at (H_e= 9 m), width (B = 18 m), and diaphragm wall length (H = 13.5 m). The excavation was simulated in three stages. Simulating two struts at the top of excavation and at a depth of 4 m is to have certain results. The structural elements (diaphragm wall and tunnel lining) were simulated as plates, **Table I**. The Poisson ratio (ν) was 0.15 and longitudinal space ($L_{spacing}$) between the struts was 4.5 m. The analysis results revealed the difference between displacement geometry for Tests (C and S), as shown in **Fig. 3**. According to test C, **Fig. 3a** clarifies the gradient in displacement around the tunnel by the effect of excavation in soil layers. Conversely, due to (test S), the tunnel left spring located beside the diaphragm wall by a distance was 1.5 m. **Fig. 3b** shows the displacement geometry by the effect of deep excavation. **Fig. 4** plots the computed results for tests C and S that were compatible with the centrifuge model. The results were represented as a relationship between δ_s/H_e and d/H_e. In test C, the values of normalized distance behind diaphragm wall (d/H_e) were 0.07, 0.5, and 0.83. The values of the normalized ground surface settlement (δ_s/H_e) were 0.1, 0.04, and 0.01. In test S, the values of normalized distance behind the diaphragm wall (d/H_e) were 0.07, 0.3, 0.75, and 1.15 and the values of the normalized ground surface settlement (δ_s/H_e) were 0.12, 0.1, 0.06, and 0.02. The tests neglected the settlement in ground surface after the distance of 1.15 H_e behind the excavation. This verification proved the compatibility between the centrifuge tests and 2D numerical analysis to validate the centrifuge model of sand soil.

Table I: Structural elements properties

Parameter	Concrete Lining d = 0.18 m	Diaphragm Walls d = 0.96 m	Struts	
			Strut 1	Strut 2
Elastic modulus of concrete, Ec (MN/m²)	35000	35000	35000	35000
Axial stiffness, EA (MN/m)	18500	453600	530	1640
Flexural rigidity, EI (MNm²/m)	50	34840	–	–
Weight, w (kN/m²)	20	40	–	–

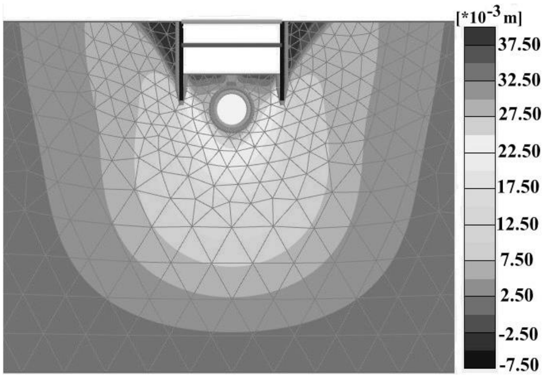

(a)

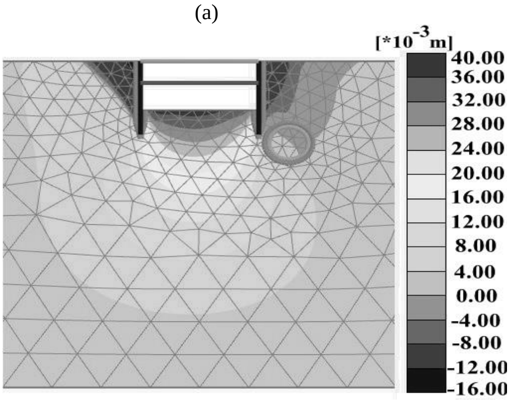

(b)

Fig. 3: Displacement geometry for the model (a) tunnel under excavation, (b) tunnel beside excavation.

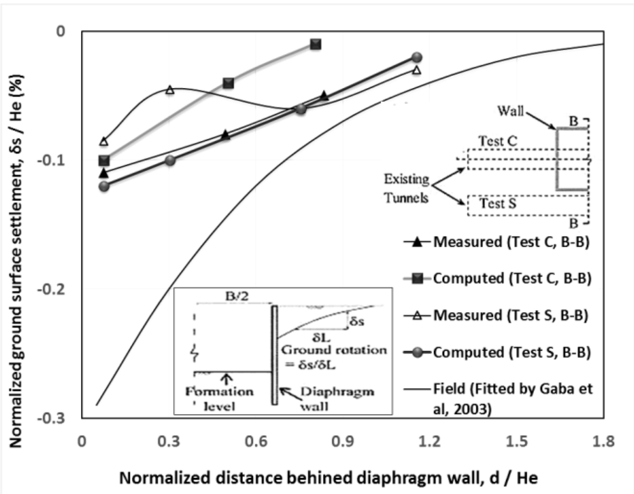

Fig. 4: Validation combined diagram for computed, field and measured centrifuge results (tests C and S).

II.3. EVALUATION OF TUNNEL MODEL IN LAYERED SOFT CLAY

The second stage of this study presents a 2D numerical analysis as plain strain analysis. This research has applied a contributed extensive study on parameters evaluated from conventional laboratory tests (i.e., triaxial and oedometer tests) by [12] on the soil of Bangkok Mass Rapid Transit (MRT) blue line project (*Sukhumvit Station*). The proposed model in this study had a deep excavation beside and above the tunnel, as illustrated in **Fig. 5**. In the case of tunnel under deep excavation, the depth of tunnel crown from ground surface is expressed as ($C = H_e + C_t$). The ground water level was at (0.00) under Made Ground layer (*MG*) that had a surface level of (+3 m). Bangkok Soft Clay (BSC) was below the (MG) layer and above the Medium Clay (MC). However, (MC) layer is above the 1st Stiff Clay (1st SC). The layer of Clayey Sand (CS) lies between (1st SC) and (2nd SC) as shown in **Fig 5a** and **Fig 5b**. The tunnel crown was leveled at three positions (3, 6, and 9 m) beside and under the deep excavation in soft soil. The excavation is by disregarding the soil layers from levels (3, 6, 9, and 12 m). PLAXIS 2D CE V20 was applied due to drainage types such as Consolidated-Undrained (CU) and Consolidated-Drained (CD). **Table II** lists the related dimensions in the model.

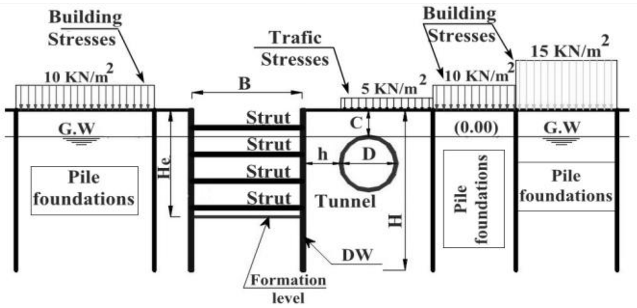

(a)

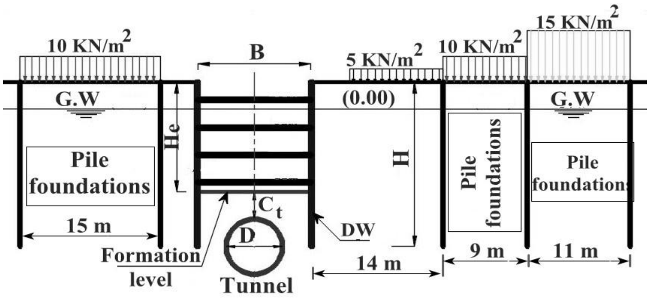

(b)

Fig. 5: The model details according to deep excavation (a) beside, and (b) above the tunnel.

Table II: The related dimensions in the proposed models.

Dimensions	Absolute Values	Related to D
H_e: Excavation depth	12.0 m	2.0 D
B: Excavation width	12.0 m	2.0 D
H: Diaphragm wall (DW) length	18.0 m	3.0 D
h: Distance between tunnel and DW	4.0 m	0.67 D

III. DATA AND ANALYSIS PROCEDURES

Sukhumvit Mass Rapid Transit (*MRT*) Station is the first underground line in Bangkok. Extensive field and experimental studies have been performed on Bangkok clay [17]. Moreover, the procedures for testing soft and stiff Bangkok clays (oedometer and triaxial) to determine the sampling stiffness and strength and evaluate the parameters of hardening soil model that have been presented [10]. Laboratory and field tests were conducted at different locations in Bangkok city [18] and the small strain stiffness of soil was determined using small strain shear modulus (G_0) and reference shear strain ($\gamma_{0.7}$). Soil properties are organized according to Plaxis requirements. Two different material models were applied:

- Mohr – Coulomb model (MC),
- Hardening Soil Model with Small Strain stiffness (HSS).

III.1. MOHR–COULOMB MODEL (MC)

Mohr–Coulomb Model (MC) is a linear elastic perfectly plastic model. It has been widely used for clayey soils in geotechnical engineering applications. Elasticity is based on Hook's law ($\sigma = E \times \varepsilon$). Plasticity based on MC failure criterion involves strains that cause deformations. The soil parameters are easy to obtain in this concept. The undrained shear strength (s_u) and undrained elastic modulus (E_u) are required for the fast-loading cases. The parameter of undrained shear strength (s_u) of the Sukhumvit sub-soils was obtained in [12] due to vane shear and triaxial tests that were used to govern the layers strength of the Bangkok Soft Clay. **Table III** lists the parameters of MC model.

III.2. HARDENING SOIL MODEL WITH SMALL STRAIN STIFFNESS (HSS)

HSS is a modification of the HS model, it incorporates the small strain stiffness of soils after [18]. Recently, it was reported [19] that the results obtained by HSS model had a greater accuracy with respect to the model dimensions. HSS model requires two main additional parameters, i.e., initial shear modulus (G_0) at very small strain and shear strain ($\gamma_{0.7}$) at the secant shear modulus (G_S) when it reduces to approximately 72.2% G_0, as shown by equations (1) and (1a).

$$G_S = 0.722\ G_0 \qquad (1)$$

$$G_0 = 1.385\ G_S \qquad (1a)$$

The relation can be expressed as equation (2).

$$G_S / G_0 = 1 / [1 + a\,(\gamma / \gamma_{0.7})] \qquad (2)$$

Where (γ) is the large shear strain and (a) is a constant (a = 0.385 when $\gamma = \gamma_{0.7}$) that will back to equation (1).

These parameters are utilized to predict the soil stiffness at small strain. The data of the small strain parameters for the *(MG)* and (*SC*) layers are limited and the expected soil movements are small in comparison with that of the (*BSC*), (*MC*), (1st *SC*), and (2nd *SC*) layers. Therefore, HS model is used in (*MG*) and (*CS*) layers, but HSS is only applied with the other layers. Accordingly, [12] presented details of small strain stiffness parameters for Bangkok clays. The parameters of HSS are presented in **Table IV**. Moreover, **Table V** presents the structural element parameters as plate elements. Temporary struts as anchors are every 4.5 m longitudinal and has an axial stiffness EA = 4440 MN/m. The piles under the raft of hypothetical buildings have axial stiffness EA =1675 MN/m. The piles foundation under proposed distributed stresses of building are simulated as anchors.

Table III: Parameters for MC Analysis

Layer	Soil type	Depth	γ_b (KN/m²)	E_u (KN/m²)	E' (KN/m²)	ν_u	ν'	Analysis type
1	MG	3 - 0	18	-	8000	-	0.3	CD
2	BSC	0 – (-12)	16.5	20500	-	0.495	-	CU
3	MC	(-12) – (-14)	17.5	27500	-	0.495	-	CU
4	1st SC	(-14) – (-20)	19.5	40000	-	0.495	-	CU
5	CS	(-20) – (-21)	19	-	53000	-	0.25	CD
6	2nd SC	(-21) – (-40)	20	72000	-	0.495	-	CU

Table III (con't): Parameters for MC Analysis

Layer	Soil type	Depth (m)	S_u (KN/m²)	Ø' (Degrees)	C' (KN/m²)
1	MG	3 - 0	-	25	1
2	BSC	0 – (-12)	20	-	-
3	MC	(-12) – (-14)	55	-	-
4	1st SC	(-14) – (-20)	80	-	-
5	CS	(-20) – (-21)	-	27	1
6	2nd SC	(-21) – (-40)	120	-	-

Table IV: Parameters of (HSS) Analysis

Layer	Soil type	Depth (m)	γ_b (KN/m³)	E_{50}^{ref} (KN/m²)	E_{oed}^{ref} (KN/m²)	E_{ur}^{ref} (KN/m²)	ν'_{ur}	Analysis type
1	MG	3 - 0	18	45600	45600	136800	0.2	CD
2	BSC	0 – (-12)	16.5	800	850	8000	0.2	CU
3	MC	(-12) – (-14)	17.5	1650	1650	5400	0.2	CU
4	1st SC	(-14) – (-20)	19.5	8500	9000	30000	0.2	CU
5	CS	(-20) – (-21)	19	38000	38000	115000	0.2	CD
6	2st SC	(-21) – (-40)	20	8500	9000	30000	0.2	CU

Table IV (con't): Parameters of (HSS) Analysis

Layer	Soil type	Depth (m)	G_0 (KN/m²)	$\gamma_{0.7}$ (%)	Ø (Degrees)	C (KN/ m²)	m	K_0
1	MG	3 - 0	-	-	25	1	1	0.58
2	BSC	0 – (-12)	10000	0.08	23	1	1	0.7
3	MC	(-12) – (-14)	12000	0.09	25	10	1	0.6
4	1st SC	(-14) – (-20)	30000	0.1	26	25	1	0.5
5	CS	(-20) – (-21)	-	-	27	1	0.5	0.55
6	2nd SC	(-21) – (-40)	50000	0.1	26	25	1	0.5

Table V: The structural element parameters as plate elements.

Parameter	**Lining d = 0.6 m**	**Diaphragm Walls d = 1.2 m**	**Building raft d = 1.0 m**
Elastic modulus of concrete, Ec (kN/m²)	24400	24400000	24400000
Axial stiffness, EA (kN/m)	14640000	29280000	24400000
Flexural rigidity, EI (kN/m²/m)	439000	3514000	2033000
Weight, w (kN/m²)	9.6	19.2	25
Poisson ratio, ν	0.2	0.2	0.2

III.3. MESH GENERATION AND BOUNDARY CONDITIONS

Fig. 6 depicts the finite element (FE) mesh in case of tunnel beside (**Fig. 6a**) and under deep excavation (**Fig. 6b**).

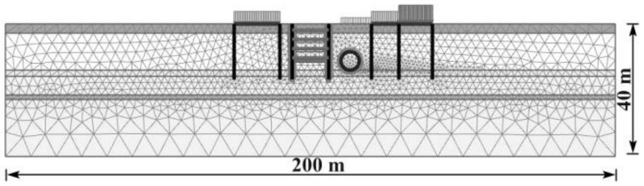

(a)

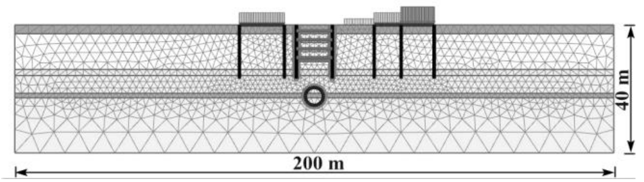

(b)

Fig. 6: FE mesh and boundary condition for the model of (a) tunnel beside, and (b) tunnel under deep excavation.

Mesh generation was selected as enhanced mesh refinement and the element distribution was the fine option. The soil was simulated as plain strain model using 15-node element. Grouting pressure (p_{ref} = -220 KN/m^2) was applied as user define in Plaxis by representing Tunnel Boring Machine (TBM) in the tunnel excavation. According to TBM, the reference value of tunnel contraction C_{ref} = 0.5 %.

IV. RESULTS OF ANALYSIS AND DISCUSSION

The models adopted verified results for the deformation of ground surface and the deformation at the invert of the tunnel cross section. The results of the analysis mainly evaluated the small strain stiffness of soil under the effect of deep excavation. The evaluation was performed by a comparison between HSS and MC. This exhibited the compatible limits between MC and HSS to determine the predicted deformation of ground surface and tunnel invert by the effect of excavation, as shown in **Fig. 7** and **8,** respectively. In the case of excavation beside the tunnel, MC presented a conceivable stability for tunnel and ground surface above. This was in contrast to the case of excavation bed above the tunnel. In the case of HSS, it adopted a similar instability behavior for the tunnel ground surface due to excavation.

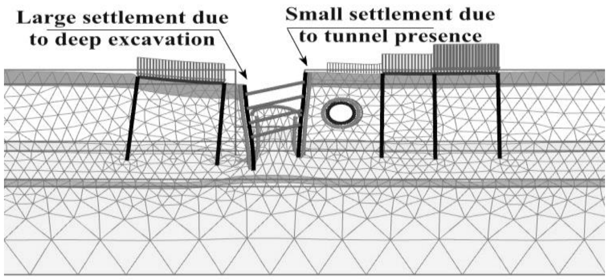

(a)

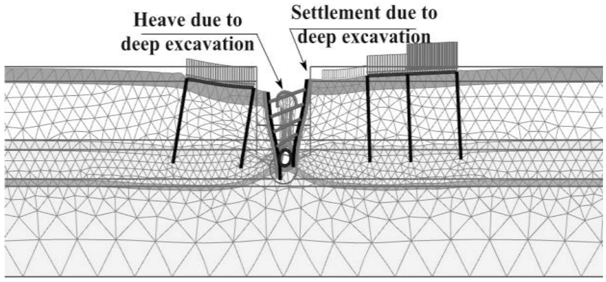

(b)

Fig. 7: Deformed shape of analyzed model by MC (a): for tunnel beside excavation (b): for tunnel under excavation.

The non-linear behavior of soil is represented by the change in soil stiffness with an increase in the stresses on soil mass. MC model works by two parts. The linear elastic part depends upon the law of isotropic elasticity. The perfectly plastic part is a constitutive model with a fixed yield surface, fixed value of stiffness, and limited in plastic strains (Under-predicted deformation).

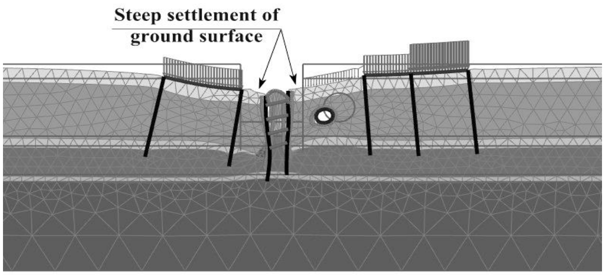

(a)

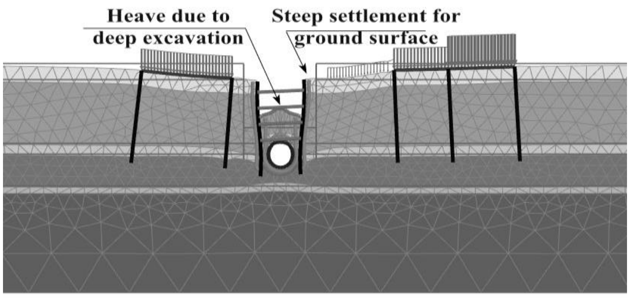

(b)

Fig. 8: Deformed shape by HSS model (a): for tunnel beside excavation (b): for tunnel under excavation.

MC model calculates stiffness (E_{50}) at elastic limits that is the ***over-predicted deformation*** of soil, **Fig. 9**. The soil reaches the plastic stage when the stresses are increased greater than 50% of soil ultimate strength, i.e., ***under-predicted deformations*** due to MC model. HSS deals with the stage of non-linear plastic behavior of soil. It incorporates the effect of deep excavation and this is considered as ***over-predicted deformation*** due to the evaluation of small strain stiffness.

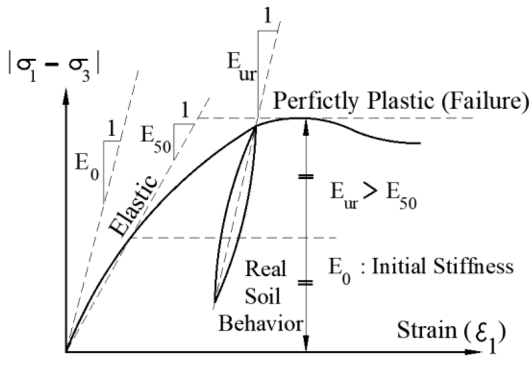

Fig. 9: Limits of Stiffness (E_{50}) due to MC model at elastic behavior of soil (drained).

IV.1. GROUND SURFACE DEFORMATION INDUCED TUNNEL PRESENCE

Before performing a close excavation and regardless of tunnel position at the mentioned levels, it was ensured that the results clarified the deformation of ground surface above tunnel under the effect of tunnel shallowness. The distance between tunnel and pile body was 2/3 D. Related to model analysis by MC, the tunnel presence beside piles and under distributed loads on surface caused a heave on the ground surface. This case was due to the following important reasons:

1) Shallowness of tunnel body owing to the small thickness of soil layer above.
2) The internal reaction of confined soil between tunnel and piles that forced the tunnel to raise the soil surface above.

It can be observed in **Fig. 10** that the measured distance on surface deformation behind the tunnel was 1.7 D. The extended heave on the ground surface above the tunnel body had a length L_h = 4.2 D. The length of the heave decreased with an increase in the tunnel depth in the soil. **Fig. 11** depicts a similar case by HSS model. Behind the tunnel, the measured distance on surface deformation was D. The extended heave on the ground surface above tunnel body had a length of L_h = 2.7 D. The study appropriately clarified when the depth of tunnels can be considered in shallow limits, particularly for the projects with similar conditions of study model. Before beginning an excavations, MC and HSS depict a same stable case for ground surface that may be at tunnel depth C ≥ 2D.

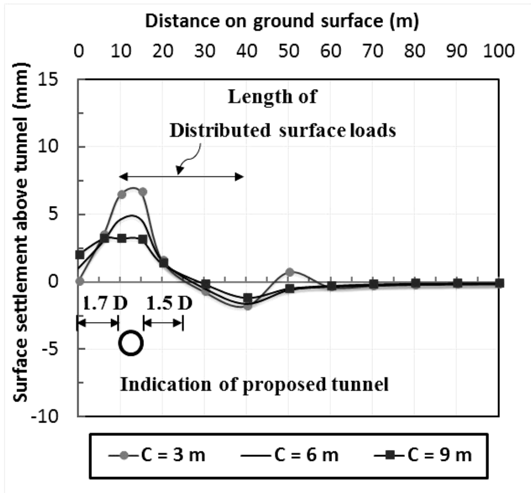

Fig. 10: Performance of ground surface above shallow buried tunnel before the beginning of the excavation beside, MC model.

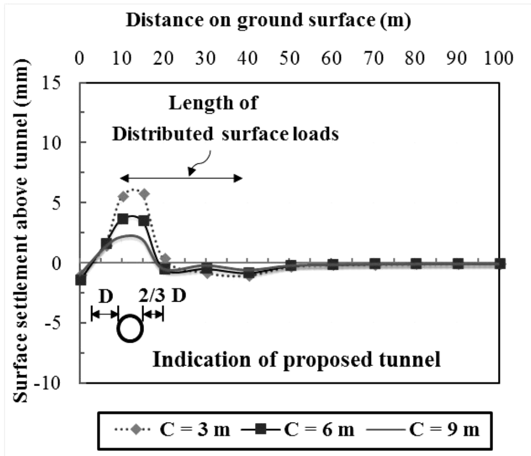

Fig. 11: Performance of ground surface above shallow buried tunnel before the beginning of excavation beside, HSS model.

IV.2. GROUND SURFACE SETTLEMENT INDUCED DEEP EXCAVATION

Beginning of the excavation (Stresses increase) beside the tunnel caused settlement due to soil drawdown behind supporting system of excavation. MC model worked under isotropic elasticity that is trying to come back at supporting system (***under-predicted deformation***) regardless excavation effect. HSS exhibited a steep and accurate behavior (***over-predicted deformation***), which was attributed to the decrease in the strength and stiffness induced strains increase with further excavation, as shown in **Fig. 12**.

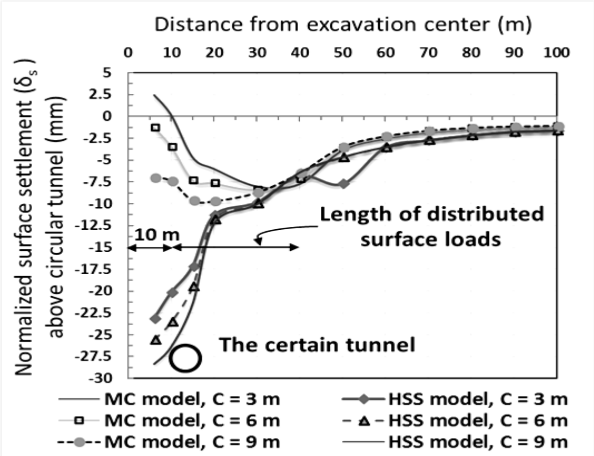

Fig. 12: Surface settlement above the tunnel by the effect of deep excavation (H_e = 12 m).

IV.3. DEFORMATIONS OF TUNNEL INVERT BESIDE DEEP EXCAVATION

The cut-off part of displacement axis represents the heave value of tunnel invert before starting excavation ($H_e/D = 0$) as shown in **Fig. 13**. The difference between the values calculated by MC and HSS increased with the beginning of the excavation process ($H_e/D > 0.5$). In the case of MC model, increasing the excavation depth ($H_e/D > 0.5$) beside the tunnel had a restricting effect on the heave of tunnel invert and the results are convergent even if the tunnel depth increased. Undefined behavior by MC model (***under predicted deformation***) for tunnel invert point beside deep excavation. The analysis by HSS presents that increasing the excavation depth ($H_e/D > 0.5$) beside the tunnel (Stress increase) adopts clear decrease in heave behavior. The lack of heave is an indicator of stiffness stability for the invert of tunnel (***over-predicted deformation***).

IV.4. VERTICAL DISPLACEMENT AT TUNNEL INVERT UNDER DEEP EXCAVATION

Excavation above buried tunnel means unloading of soil over the tunnel. Unloading the soil above causes displacement and decreases the buried tunnel stability. In addition, removing amounts of soft soil above buried tunnel is comparatively critical than that of unloading the soil beside tunnels. This is according to the thickness of soil layer between the formation level of excavation and tunnel crown (C_t). This study measured the vertical displacement of tunnel invert point under excavation levels. It can be observed in **Fig. 14a** that at C_t = 3 m under formation level of excavation (soil unloading), the analysis by HSS or MC calculated critical heave for the invert of tunnel lining when (H_e = 2D). The small cut-off part of displacement axis represents the heave values at the invert point before starting excavation above the tunnel. The difference between the values calculated by MC and HSS increased after beginning the excavation process ($H_e/D > 0.5$), as shown in **Fig. 14b**. Increasing the excavation depth (H_e) increases the vertical heave of tunnel invert point. According to HSS analysis, the heave is smaller than that by MC model, and tends to be linear by increasing the invert depth of tunnel, as shown in **Fig. 14c**. A difference between the results of MC was not observed. This indicated that the difference between MC and HSS values increased with an increase in the excavation depth (H_e > 2D) and the depth of tunnel invert point.

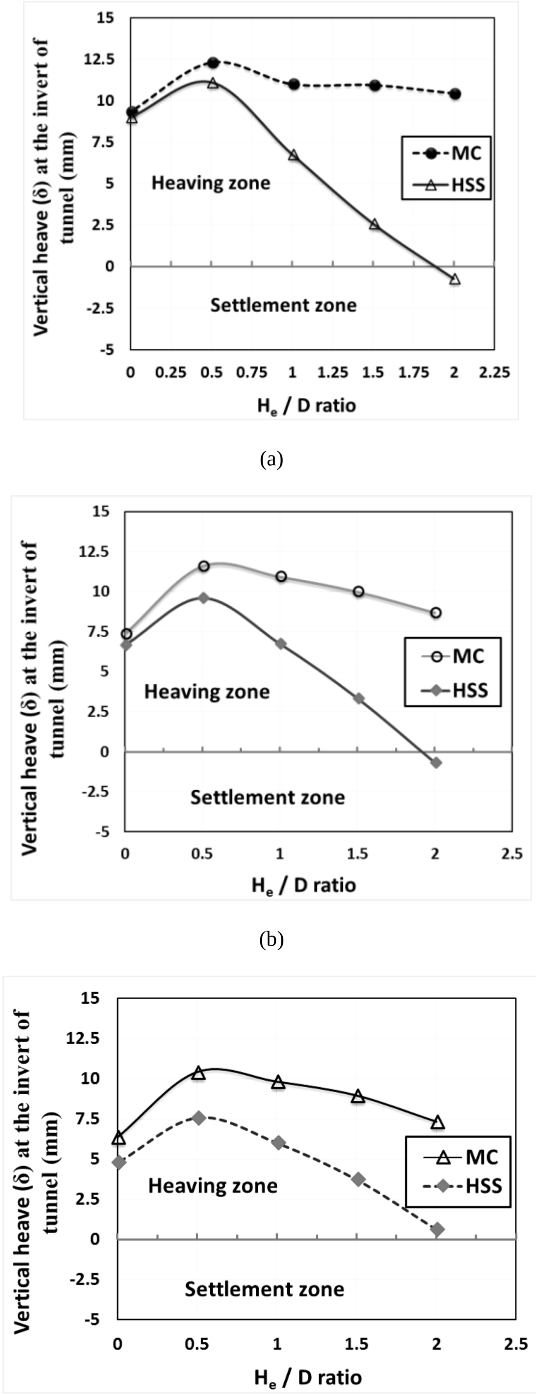

Fig. 13: Heave at tunnel invert, (a): C = 3 m, (b): C = 6 m and (c): C = 9 m due to MC and HSS models by increasing excavation depth.

IV.5. EFFECT OF TUNNEL-EXCAVATION AREA RATIO

This study adopts a reliable approach that depicts the importance of evaluating tunnel displacement by joining tunnel cross sectional area by the above cross sectional area of excavation. It is stated that the circular tunnel – excavation area ratio as a factor named Effective Area Ratio (R) and it is an innovative addition to be considered when achieving new deep excavation above existed tunnel.

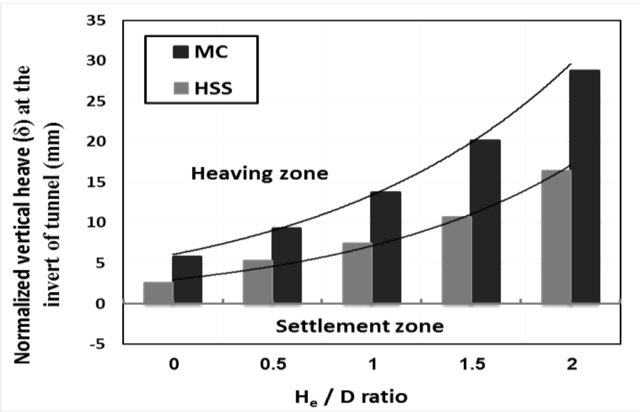

(a)

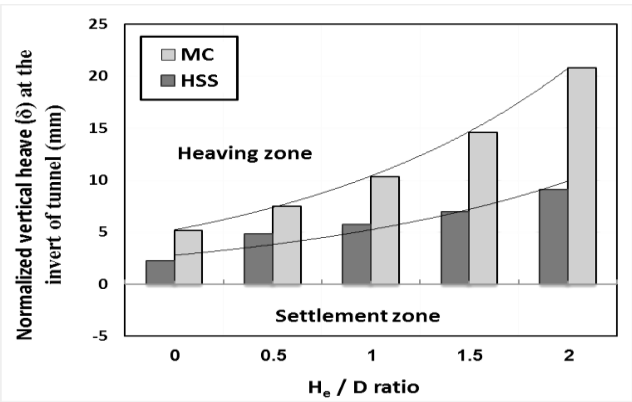

(b)

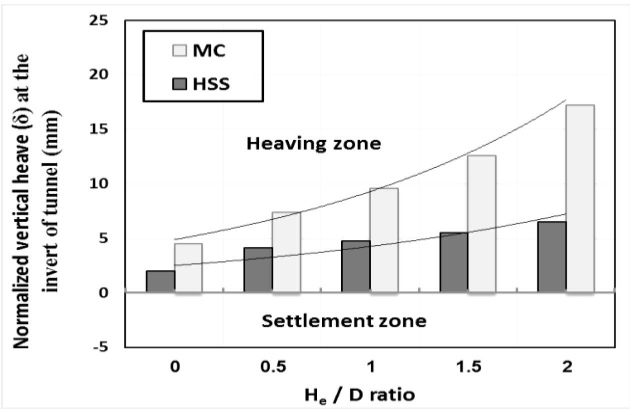

(c)

Fig. 14: Heave displacement by MC and HSS models at tunnel invert under excavation increase (a) at C_t = 3 m, (b) at C_t = 6 m, and (c) at C_t = 9 m.

Assuming the sectional area of excavation A_E due to equation (3).

$$A_E = B \times H_e \tag{3}$$

The tunnel sectional area is A_T as in equation (4).

$$A_T = \pi D^2 \tag{4}$$

Where, B and H_e are the excavation dimensions, and D is the tunnel diameter. Therefore, (R) is obtained by equation (5).

$$R = A_E / A_T \tag{5}$$

It can be observed in **Table VI** that connecting the last assumptions in relation is to stand on the effect of increasing excavation sectional area on the value of area ratio (R) that is inversely proportional to the sectional area of tunnel.

Table VI: Tunnel-excavation sectional area and (R).

A_T (m^2)	B (m)	H_e (m)	A_E (m^2)	R
		0	0	0
		0.5 D	1.0 D^2	0.32
3.14 D^2	2 D	1.0 D	2.0 D^2	0.64
		1.5 D	3 D^2	0.96
		2.0 D	4 D^2	1.27

Table VII elaborates the association between R and the corresponding values of tunnel heave (δ) using MC and HSS models. **Fig. 15** plots the non-linear relationship between effective area ratio (R) and maximum tunnel heave by the variation of tunnel depth. Increasing R-values increases the heave of tunnel body. However, the mentioned variable depths of tunnel decrease the tunnel heave. In addition, tunnel sectional area (A_T) is inversely proportional to the heave value of the tunnel.

A mathematical formula was developed to calculate R at variable depths of excavation according to the diameter of the underneath tunnel. The relationships in **Fig. 14** and **15** were based on equations (6), (7), (8), (9) and (10). Therefore, it is possible to obtain the values of δ from **Fig. 15** during excavation that correspond to the calculated values of R ratio.

$$\textbf{Fig. 14} \text{ represented that } H_e / D \propto \delta \tag{6}$$

$$\textbf{Fig. 15} \text{ represented that } R \propto \delta \tag{7}$$

$$R = (B \times H_e) / \pi D^2 = \text{constant} \times (H_e / D) \tag{8}$$

$$R = (B / \pi D^2) \times (H_e / D) \tag{9}$$

$$R = 0.64\,(H_e / D) \tag{10}$$

Table VII: Effective Area Ratio (R) and the associated heave by MC and HSS analysis

Model	Relationship	Tunnel depth C_t under formation level of excavation														
		0.5 D					1.0 D					1.5 D				
MC	R	0	0.32	0.64	0.96	1.27	0	0.32	0.64	0.96	1.27	0	0.32	0.64	0.96	1.27
	Tunnel heave (mm)	5.8	9.3	13.8	20.2	28.8	5.2	7.5	10.4	14.6	20.9	4.5	7.42	9.56	12.63	17.2
HSS	R	0	0.32	0.64	0.96	1.27	0	0.32	0.64	0.96	1.27	0	0.32	0.64	0.96	1.27
	Tunnel heave (mm)	2.6	5.37	7.52	10.7	16.5	2.24	4.8	5.7	7	9	2	4.1	4.76	5.5	6.5

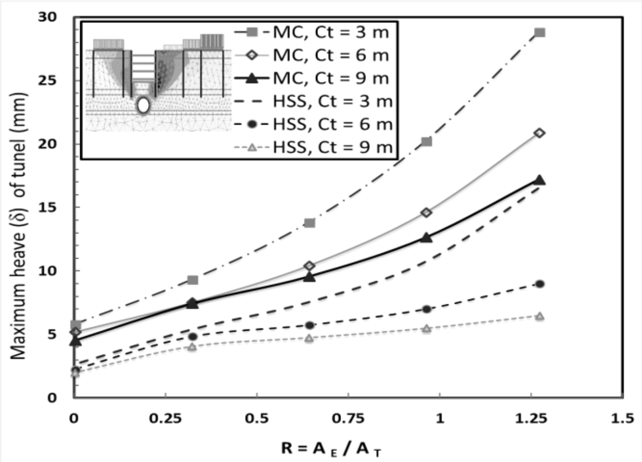

Fig. 15: The relationship between effective area ratio (R) and tunnel maximum heave with the change of tunnel depth - MC and HSS models.

V. CONCLUSION

The results of the numerical analysis summarized a convenient ideal comprehension for the effect of excavation on the soil strain-stiffness. 2D numerical analysis was used to validate the results of centrifuge model tests. In addition, this study concluded that:

- MC model cannot adopt the real case of tunnel invert point by the effect of deep excavation (***under-predicted deformation***). However, HSS accurately assessed steeper accurate behavior as ***over-predicted deformation*** and this was useful for design precautions.
- Handling of stiffness at small strain is more applicable by HSS model in predicting the deformations of facilities under a variable behavior of soft soil.
- Before beginning a new excavations, stable case for ground surface above is possible when tunnel depth ($C \geq 2$ D).
- Mathematical formula for R is accurate to determine the related value of tunnel heave (δ) using the (R–δ) relationship.

ACKNOWLEDGMENT

The authors are grateful to Assiut, Sohag, and Al-Azhar Universities for providing scientific and technical support during the research.

REFERENCES

[1] Abd-Elnaiem M. A., "Improving Behavior of Tunnel Lining Constructed in Layered Soil Including Soft Clay Layer Using Stone Columns". Arab Journal of Science Eng.; vol. 38, pp. 3289–3300, 2013. Available: https://doi.org/10.1007/s13369-013-0650-x.

[2] Komiya K., Soga K., Akagi H., Hagiwara T., Bolton M. D., "Finite Element Modelling of Excavation and Advancement Processes of a Shield Tunnelling Machine". Soils and Foundations; vol. 39, no. 3, pp. 37–52, June 1999. Available: https://doi.org/10.3208/sandf.39.3_37.

[3] Juneja A., Hegde A., Lee F.H., Yeo C.H., "Centrifuge modelling of tunnel face reinforcement using forepoling". Tunnelling and Underground Space Technology; vol. 25, pp. 377–381, 2010. Available: https://doi.org/10.1016/j.tust.2010.01.013.

[4] Chang Ch.T., Sun Ch.W., Duann S.W., Hwang R. N., "Response of a Taipei Rapid Transit System (TRTS) tunnel to adjacent excavation". Tunnelling and Underground Space Technology; vol. 16, pp. 151–158, 2001. Available: https://doi.org/10.1016/S0886-7798(01)00049-9.

[5] Demagh R., Emeriault F., Mahmoud F., "3D Modelling of Tunnel Excavation Using Pressurized Tunnel Boring Machine in Overconsolidated Soils". Geotechnical and Mechanical studies (Studia Geotechnica et Mechanica); vol. xxxv, no. 2 , pp. 3–17, 2013. Available: https://doi.org/10.2478/sgem-2013-0020.

[6] Liu H., Li P., Liu J., "Numerical investigation of underlying tunnel heave during a new tunnel construction". Tunnelling and Underground Space Technology; vol. 26, pp. 276–283, 2011. Available: https://doi.org/10.1016/j.tust.2010.10.002.

[7] Xiao X., Chen J.J., ASCE A.M., Li M.G., Wang J.H. "Field Monitoring of an Existing Cut-and-Cover Tunnel between Two Large-Scale Deep Excavations". Journal of Aerospace Engineering; vol. 31, no. 6, pp. 04018082-1 - 04018082-13, July 11, 2018. Available: https://doi.org/10.1061/(asce)as.1943-5525.0000851.

[8] Finno R. J., Clough G. W., "Evaluation of soil response to EPB shield tunneling". Journal of Geotechnical Engineering; vol. 111, no. 2, pp. 155–173, February 1985. Available: https://doi.org/10.1061/(ASCE)0733-9410(1985)111:2(155).

[9] Likitlersuang S., Chheng Ch., Surarak Ch., Balasubramaniam A., "Strength and stiffness parameters of Bangkok clays for finite element analysis". Geotechnical Engineering Journal of the SEAGS & AGSSEA; vol. 49, no. 2, pp. 150–156, June 2018.

[10] Surarak Ch., Likitlersuang S., Wanatowski D., Balasubramaniam A., Oh E., Guan H., "Stiffness and strength parameters for hardening soil model of soft and stiff Bangkok clays". The Japanese Geotechnical Society, Journal of Soils and Foundations; vol. 52 no. 4, pp. 682–697, 2012. Available: https://doi.org/10.1016/j.sandf.2012.07.009.

[11] Schanz T, Vermeer P.A., Bonnier P.G., "The hardening soil model: Formulation and verification". Taylor & Francis group, Beyond 2000 Computational Geotechnics – First Eddition, Routledge, 16 pages, 1999. Available: https://doi.org/10.1201/9781315138206-27.

[12] Likitlersuang S., Surarak Ch., Wanatowski D., Oh E., Balasubramaniam A. "Finite element analysis of a deep excavation: A case study from the Bangkok MRT". Journal of Soils and Foundations; vol. 53, no. 5, pp. 756–773, 2013.

[13] Charles W.W. Ng, Boonyarak Th., Mašín D., "Three-dimensional centrifuge and numerical modeling of the interaction between

perpendicularly crossing tunnels". Canadian Geotechnical J.; vol. 50, pp. 935–946, July 2013. https://doi.org/10.1139/cgj-2012-0445.

[14] Karakus M., Fowell R.J., "Effects of different tunnel face advance excavation on the settlement by FEM". Tunnelling and Underground Space Technology; vol. 18, pp. 513–523, 2003. Available: https://doi.org/10.1016/S0886-7798(03)00068-3.

[15] Charles W.W. Ng, Shi J., Hong Yi, "Three-dimensional centrifuge modelling of basement excavation effects on an existing tunnel in dry sand". Canadian Geotechnical J.; vol. 50, pp. 874–888, June 2013. Available: https://doi.org/10.1139/cgj-2012-0423.

[16] Tatsuoka F.; Goto S., Sakamoto M., "Effect of some factors in strength and deformation caracterestics of sand at low pressures". Soils and foundations; vol. 26 no. 1, pp. 105–114 March 1986. Available: https://doi.org/https://doi.org/10.3208/sandf1972.26.105.

[17] Shibuya S, Tamrakar S.B., Theramast N., "Geotechnical site characterization on engineering properties of Bangkok clay". Geotechnical Engineering Journal; vol. 32 no. 3, pp. 139–151, December, 2001.

[18] Likitlersuang S, Teachavorasinskun S, Surarak Ch., Oh E., Balasubramaniam A., "Small strain stiffness and stiffness degradation curve of Bangkok Clays". Soils and Foundations; vol. 53, pp. 498–509, 2013. Available: https://doi.org/10.1016/j.sandf.2013.06.003.

[19] Brinkgreve R.B.J., Bakker K., Bonnier P., "The relevance of small-strain soil stiffness in numerical simulation of excavation and tunnelling projects". Numerical Methods of Geotechnical Engineering, Schweiger (ed.), Taylor & Francis group, pp. 133–139, 2006.

Ahmed Kamal M. Ibrahim worked as an assistant lecturer in the Civil Engineering Department at the University of Al-Azhar, Qena, Egypt. He is a member in IAENG.

Master Science in Geotechnical Engineering, 2018. The study were about supporting sand slopes by piles conducted from sand and Gravels soil cemented by cement kiln dust and reinforced by Monofilament Glass Fiber.

He is a Candidate of Doctoral Philosophy in tunnels at University of Assiut, Egypt. His research interests include Soil investigations and tunnels simulation and analysis. The author published many researches in slope improvement, such as a research entitled "Effect of glass fiber on sand – gravel soil mixture stabilized by cement dust". Achieving a study of 2D numerical analysis on piles performance in sand slope under variable conditions. In addition to numerical studies for the internal stresses in tunnel lining by the effect of close deep excavation to help in predicting the behavior of tunnel lining and design.

Abd-Elaziz Ahmed Senoon is a Professor in the Civil Engineering Department at the University of Assiut, Egypt. Master Science in Geotechnical Engineering, 1994. Doctoral Philosophy from University of Charles Prague, Czech Republic, 2001.

Since 2001, he has presented many lectures in soil mechanics and foundations engineering and has attended many of conferences. He has supervised several masters and doctoral theses and arbitrated many of studies. His research interests include Soil reinforcement, numerical simulation and analysis for encased piles, soil mechanics and foundation, tunnels. The author published many researches such as a research entitled "Ultimate seismic bearing capacity of strip footing using modified Krey's methods (friction circle method)".

Mamdouh Abbas Kenawi is an assistant Professor in the Civil Engineering Department at the University of Sohag, Egypt.

Master Science in Geotechnical Engineering, 1998. The study were about the Effect of Oil Contamination on some Engineering Properties of Soil.

Doctoral Philosophy under joint supervision between University of Innsbruck, Austria and University of Assiut, 2004. The study was about underground structures in consolidated clay. His research interests include soil mechanics and foundation, underground structures, and Foundation design. Since 2004, he has presented many lectures in soil mechanics and foundations engineering and has attended many of conferences. He has supervised several masters and doctoral theses and arbitrated many.

Ahmed Rushdy Towfeek is an assistant Professor in the Civil Engineering Department at the University of Al-Azhar, Qena, Egypt.

Master Science in Geotechnical Engineering from University of Assiut, Egypt, 2006. The study were about supporting pile resistance using Osterberg Cell.

Doctoral Philosophy in sand supporting by cement kiln dust from University of Assiut, Egypt, 2012. His research interests include Soil supporting and reinforcement. The author published many researches in slope improvement, such as a research entitled "Numerical analysis of concrete solider pile with steel sheet pile lagging supporting system in sandy soil". In addition "2D Numerical study on piles performance in sand slope under variable conditions".

Mostafa Abdo Abd- Elnaiem is a Professor in the Civil Engineering Department at the University of Assiut, Egypt.

Master Science in Geotechnical Engineering, 1995. The study were about the Distribution of Earth Pressure on Caissons and Shells.

Doctoral Philosophy was in tunnels and it was from University of Innsbruck, Austria, 2003.

Since 2003, he has presented many lectures in soil mechanics and foundations engineering and has attended many of conferences. He has supervised several masters and doctoral theses and arbitrated many studies.

His research interests include soil mechanics and foundation, tunnels simulation and analysis, and Foundation design. The author published many researches in tunnels such as a research entitled "Improving Behavior of Tunnel Lining Constructed in Layered Soil Including Soft Clay Layer Using Stone Columns". In addition to "Behavior of existing tunnel due to the construction of a new tunnel passed parallel under it"